



**RESEARCH ARTICLE - PHYSICS**

## Study the effect of electrode configuration and applied voltages on dielectric barrier discharge plasma performance

Hussein Galib Hassan<sup>1\*</sup>, Intesar Hato Hashim<sup>1</sup>

<sup>1</sup> Department of Physics, College of Education, Mustansiriyah University, Baghdad-Iraq

\* Corresponding author: [hussein\\_ghalib@uomustansiriyah.edu.iq](mailto:hussein_ghalib@uomustansiriyah.edu.iq)

Article Info.	Abstract
<p><i>Article history:</i></p> <p>Received 28 May 2024</p> <p>Accepted 28 June 2024</p> <p>Publishing 30 March 2025</p>	<p>This study used two custom dielectric barrier discharge plasma (DBDP) systems designs to produce non-thermal plasma and investigate its properties. The setup included two identical parallel copper electrodes with specific design dimensions (16cm length, 3 mm diameter) and two similar glass tubes (13 cm length, 5.5 mm outer diameter, and 5mm inner diameter) as a dielectric barrier. In the first design, only one of the copper electrodes was covered with a glass tube, while in the second, each one was covered with a glass tube. The optical emission spectroscopy (OES) technique was employed to analyze the produced plasma spectrum and then calculate the plasma parameters (electron temperature, electron density, frequency of electron, Debye length, and Debye number) at different conditions of <math>A_c</math> applied voltage (18-22 kV) and discharge gap distance is fixed (4 mm) for both designs. For all operating conditions, electron temperature was 4.177- 4.273 eV, while electron density was <math>1.582 \times 10^{18}</math>-<math>1.942 \times 10^{18}</math> cm<sup>-3</sup>. The results reveal a novel and significant effect of electrode configurations on the properties of the produced plasma due to the distribution of the electric field in the discharge region, sparking new avenues for research in this field.</p>

This is an open-access article under the CC BY 4.0 license (<http://creativecommons.org/licenses/by/4.0/>)

*The official journal published by the College of Education at Mustansiriyah University*

**Keywords:** Dielectric barrier discharge, Non-thermal plasma, Electrode configuration, Boltzmann plot, Plasma parameters.

### Introduction

Recently, non-thermal atmospheric pressure plasmas have gained popularity as a tool for many applications in the fields of medicine [1], [2] environment [3], [4] and agriculture [5], [6]. Furthermore, due to the lower surface damage and shallow surface penetration depth caused by non-thermal plasma, it is preferred for material processing applications and surface modification [7], [8]. Non-thermal plasmas are commonly produced by various types of electrical discharges and are described as partially ionized gases containing charged and neutral particles, as well as photons emitted when electrically excited molecules dissociate [9]. When the temperature of electrons in the plasma medium is much higher than that of neutral gases and ions, the plasma is called non-thermal plasma [10].

Dielectric barrier discharge (DBD) is a widely used discharge system that plays a crucial role in generating non-equilibrium plasma at atmospheric pressure. This system is known for its ability to produce plasma with lower power and cost [11].

Alternating current (AC) discharge is generated by applying a periodic electric field between two electrodes, where one (or both) electrodes are covered with a dielectric material such as glass or quartz to suppress large discharge currents [12]. The discharge electrodes are an essential component of DBD plasma, so the material, shape and configuration of these electrodes play an indispensable role in the characteristics of the generated plasma [12], [13].

Electron temperature and electron density are the main parameters characterizing the resulting plasma; there are many ways to estimate these parameters, some of which are direct, such as the Langmuir probe, which provides spatially accurate measurements, while other probes are indirect, such as optical emission spectroscopy (OES) [14], that used in present study. Compared to direct methods, OES is a spectroscopic method that can analyze plasma spectra without causing any interference in the plasma medium [14], [15].

Boltzmann plots are a simple and widely used method. It relies on analysis of the optical radiation released by the plasma to estimate the electron temperature. The Boltzmann diagram method is effective under local thermal equilibrium (LTE) conditions [13], [14].

Based on OES spectral analysis  $T_e$ , can be calculated using the Boltzmann relation expression [15]:

$$\ln \left( \frac{\lambda_{ji} I_{ji}}{hc A_{ji} g_{ji}} \right) = \frac{-1}{k T_e} (E_j) + \ln \left( \frac{N}{U(T)} \right) \quad (1)$$

where  $\lambda$ : is represent the wavelength,  $I_{ji}$ : is the relative intensity of the emission line among the energy levels (j and i),  $A_{ji}$  : is the transition probability of spontaneous radiative emission from the level j to the lower level i,  $g_j$  :is the statistical weight of the emitting upper level j of the studied transition,  $E_j$  : is the energy of excitation, k: is the Boltzmann constant and C: is constant.

Another important parameter is the electron number density, which describes the plasma environment and establishes its equilibrium status, usually measured from the Stark broadening. It can be determined from the line width as follows [16]:

$$n_e = \left( \frac{\Delta\lambda}{2\omega_s} \right) N_r \quad (2)$$

where  $\Delta\lambda$  is the line full width at half maximum (FWHM), and  $\omega_s$  is the theoretical line full-width Stark broadening parameter,  $N_r$  is the reference electron density equal to  $10^{16} \text{ cm}^{-3}$  for neutral atoms and  $10^{17} \text{ cm}^{-3}$  for single charged ions [16].

The plasma frequency  $f_p$  of the electrons can be calculated from [17]:

$$f_p = \left( \frac{n_e e^2}{\epsilon_0 m_e} \right)^{1/2} \quad (3)$$

where  $f_p$  Plasma frequency of electron,  $\epsilon_0$  Permittivity of free space,  $n_e$  Electron density, e Electron charge, and  $m_e$  Electron mass.

Another key parameter is the Debye length or Debye shielding, which gives the plasma quasi-neutral properties, in which the charged particles in the plasma interact with each other to reduce the effects of the generated electric fields. The Debye length can be defined as [18]:

$$\lambda_D = \left( \frac{k T_e \epsilon_0}{n_e e^2} \right)^{1/2} \quad (4)$$

The existence of plasma needs to meet basic conditions; the first condition is  $\lambda_D \ll L$ ,  $\lambda_D$  represents the system size (cm). The second condition  $N_D \gg 1$ ,  $N_D$  is Debye number (particle number density on the Debye surface), as follows [18]:

$$N_D = \frac{4\pi}{3} n_e \lambda_D^3 \quad (5)$$

The purpose of this study is to investigate the effect of customized electrode configurations on the performance of non-thermal DBD plasmas under different operating conditions.

## Experimental setup

In the present study, as shown in Fig.1, the non-thermal DBD plasma system at atmospheric pressure consists of two parallel identical copper electrodes (16 cm length, 3 mm diameter) separated by an air distance and a glass tube (13 cm length, 5.5 mm outer diameter, and 5 mm inner diameter) as a dielectric barrier to prevent electric spark formation between electrodes, see Fig. 2. In the first design as shown in Fig. 3 a, only one of the copper electrodes was covered with a glass tube, while in the second as shown in Fig.3 b, each copper electrode covered with a glass tube.

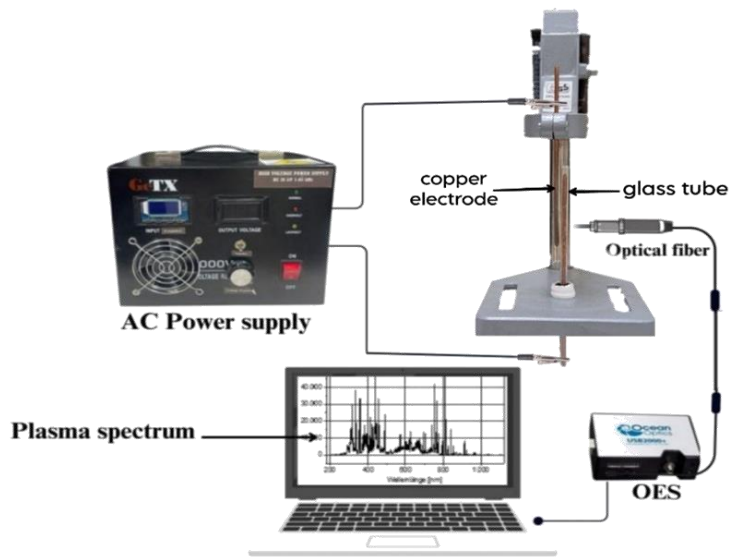


**Figure 1:** Schematic of used system setup.

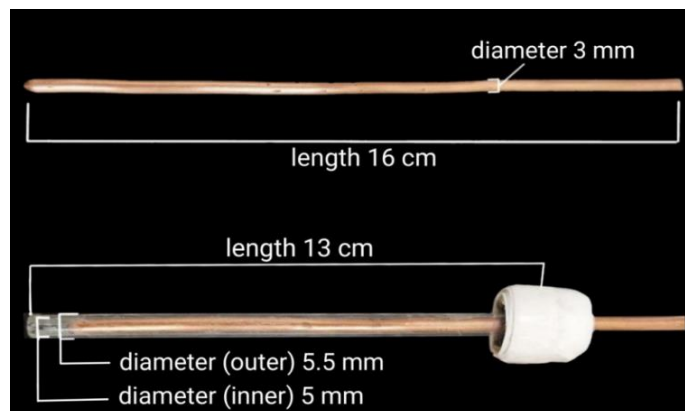


**Figure 2:** Schematic of the used electrodes.

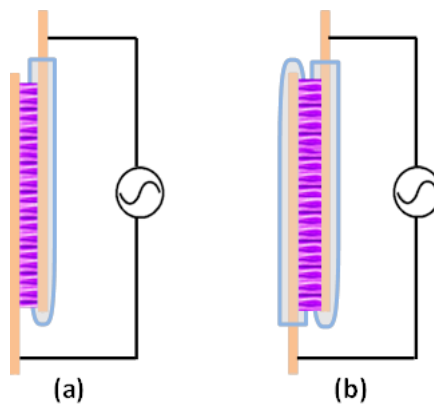


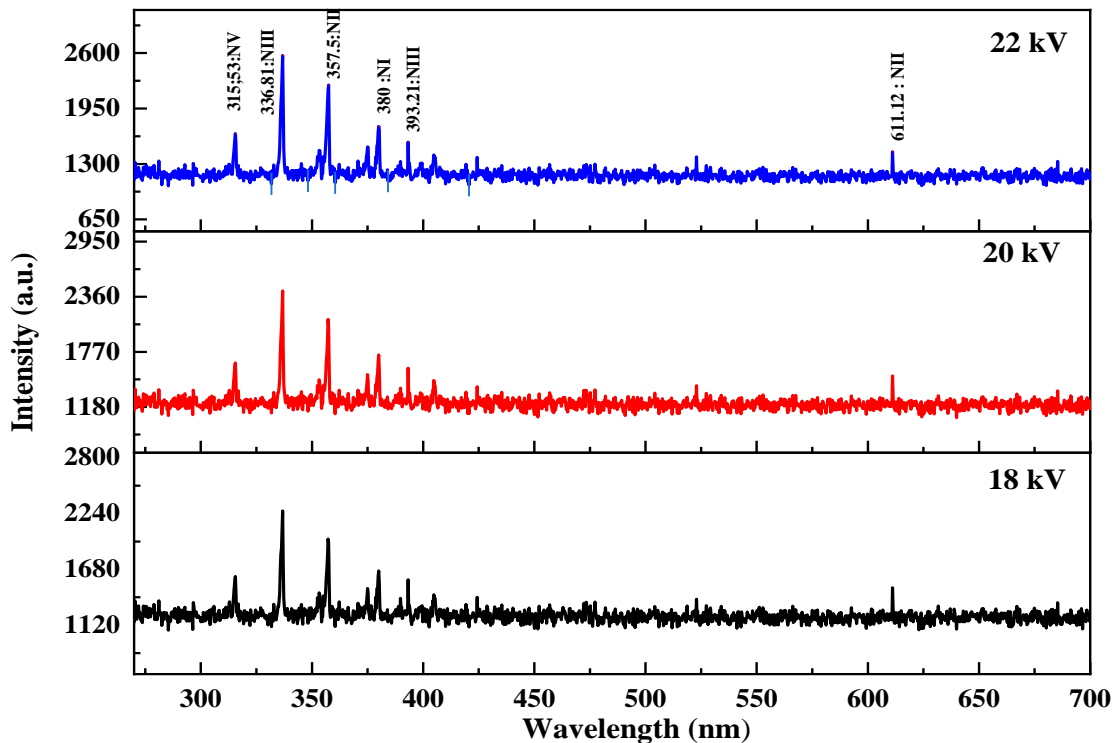
**Figure 3:** Electrodes configuration.

The two electrodes for each design were connected to an AC high-voltage power supply (fabricated indigenously), changed by 18-22 kV range, at a constant frequency of 8 kHz. The (HR4000CG-UV-NIR, Ocean Optics) optical emission spectrometer was used to analyse the plasma spectrum emitted in the discharged gap between the electrodes changed by 5 mm

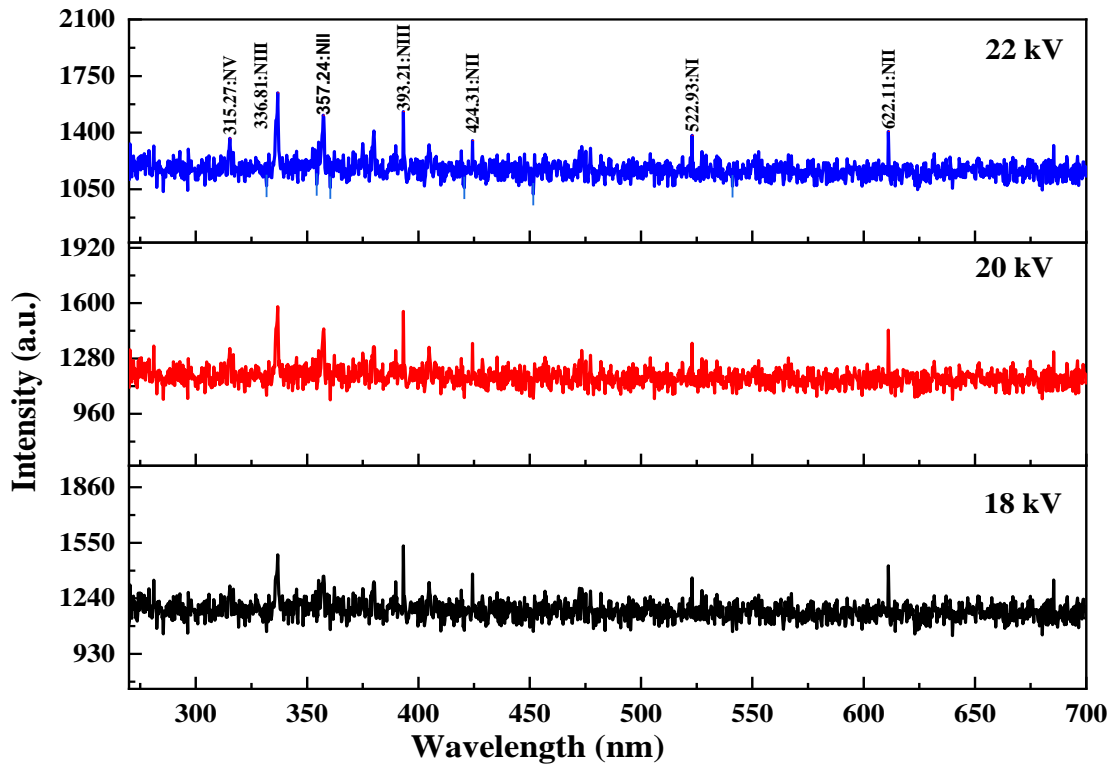
## Results

Fig. 4 and 5 show the emission spectrum of DBD plasma produced at different applied voltages (18, 20, 22 kV) at a constant distance discharge gap of 5 mm for both designs (one glass tube and two glass tubes). The distribution of intensity lines in the present system was at a wavelength range of 200 - 800 nm; according to the NIST database, all measured spectral intensity lines belong to nitrogen ions of NIII and NV [19].

For both designs, the intensity of spectral lines increased by increasing the applied voltage due to the increased electric field in the discharge gap. The rising electric field led to more collisions, consequently increasing the ionization of the nitrogen molecules in the surrounding region, leading to a higher density of charged particles and higher plasma spectrum intensity [20]. The same figures show that the intensity of DBD plasma produced in the design of one glass tube is more than that for the design of two glass tubes due to the presence of two layers of dielectric materials represented by the glass, which reduces the intensity of the electric field between discharge electrodes. Two dielectric barriers might result in a more even electric field distribution between the electrodes. That results in a more stable and homogenous plasma discharge, reducing the probability of arcing and filamentation [21], [22] .



**Figure 4:** Spectrum of DBD plasma at different at different applied voltage (One glass tube)



**Figure 5:** Spectrum of DBD plasma at different at different applied voltage (Two glass tubes).

Fig. 6 and 7 display images of the plasma spectra indicated in Fig. 4 to 5. These images illustrate the distribution of the produced plasma across the discharge gap for different voltage and gap distance conditions. The DBD plasma appears as delicate filaments, filling the gap between electrodes. The diverging and converging of these filaments refers to the density of the plasma. For both designs, the plasma became more uniform at higher voltages and spread over larger areas across the discharge gap.

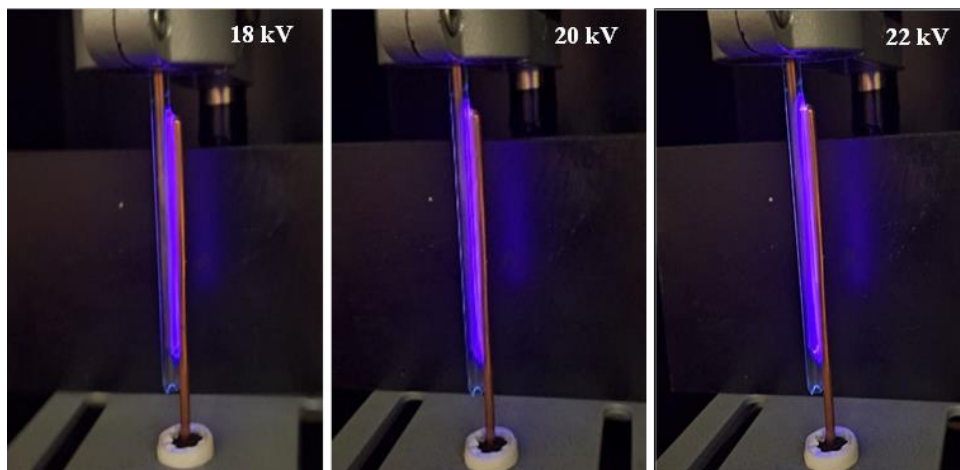


**Figure 6:** DBD plasma images at different applied voltages (One glass tubes).

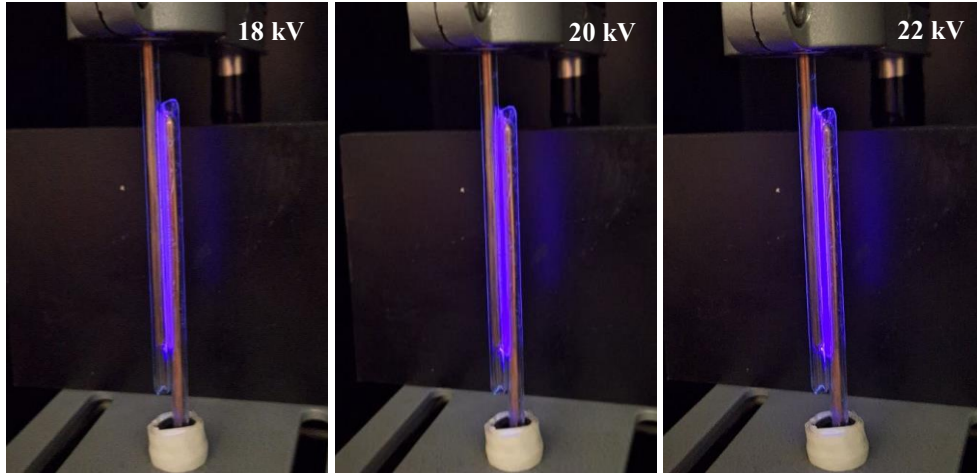


**Figure 7:** DBD plasma images at different applied voltages (Two glass tubes).

Figs 8 to 10 demonstrate the results of calculating the plasma electron temperature at different conditions of applied voltage. Plasma electron temperature represents one important characteristic of the plasma, According to the Boltzmann plot, it equals the inverse slope of the relationship between  $\ln\left(\frac{\lambda_{ji}I_{ji}}{hcA_{ji}g_{ji}}\right)$  and the upper energy level  $E_j$ . All calculated electron temperatures of the produced plasma at different applied voltage conditions for both designs are listed in Table 1.

All calculated electron temperatures of the produced plasma at different applied voltage conditions for both designs are listed in Table 1.

The results show a close correlation between plasma intensity and corresponding electron temperature. As the intensity of plasma spectrum lines increases, electron temperature rises due to the acceleration of the electrons after they are exposed to a high electric field, which leads to an increase in their kinetic energy and, consequently, temperature [21]. The increasing electric field occurs when the applied voltage increases. Plasma electron temperatures for two glass tube designs show a decrease in temperature compared to one glass tube design due to a reduction in the electric field, as explained previously.

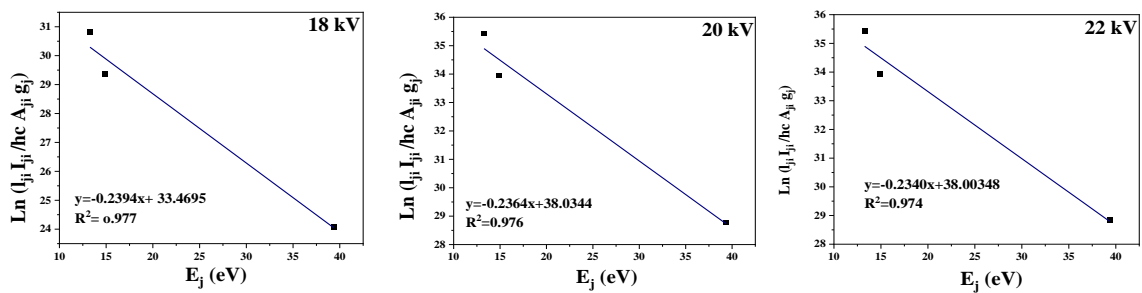


**Fig. 8:** Boltzmann diagram at different applied voltages (One glass tube)

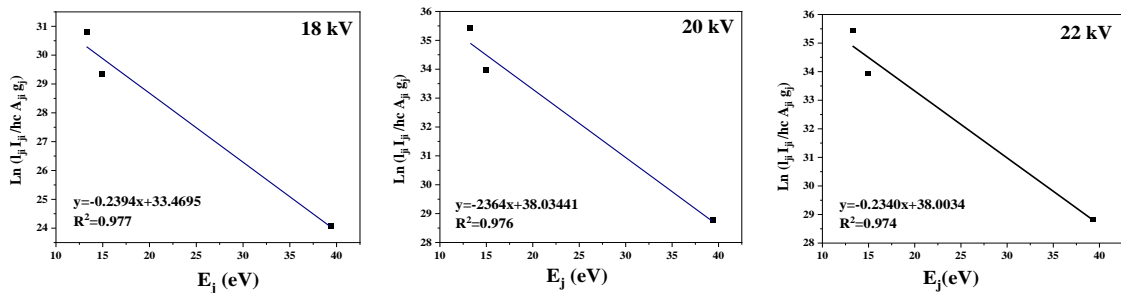


**Figure 9:** Boltzmann diagram at different applied voltages (Two glass tubes).

Figures 14 and 15 illustrate the behavior of electron temperature ( $T_e$ ), electron density ( $n_e$ ), frequency of electron ( $f_p$ ), Debye length ( $\lambda_D$ ) and Debye number ( $N_D$ ) of generated plasma at different conditions of applied voltage. The electrode configuration influences the properties of the produced plasma by changing the distribution and uniformity of the electric field and, consequently, the energy distribution of electrons in the plasma zone. Therefore, all plasma parameters are sensitive to changes in electrode design.

Electron density and electron frequency increase by increasing the electric field [21], which occurs by increasing the applied voltage, as clear in the Figures. In contrast, the Debye length and Debye number.

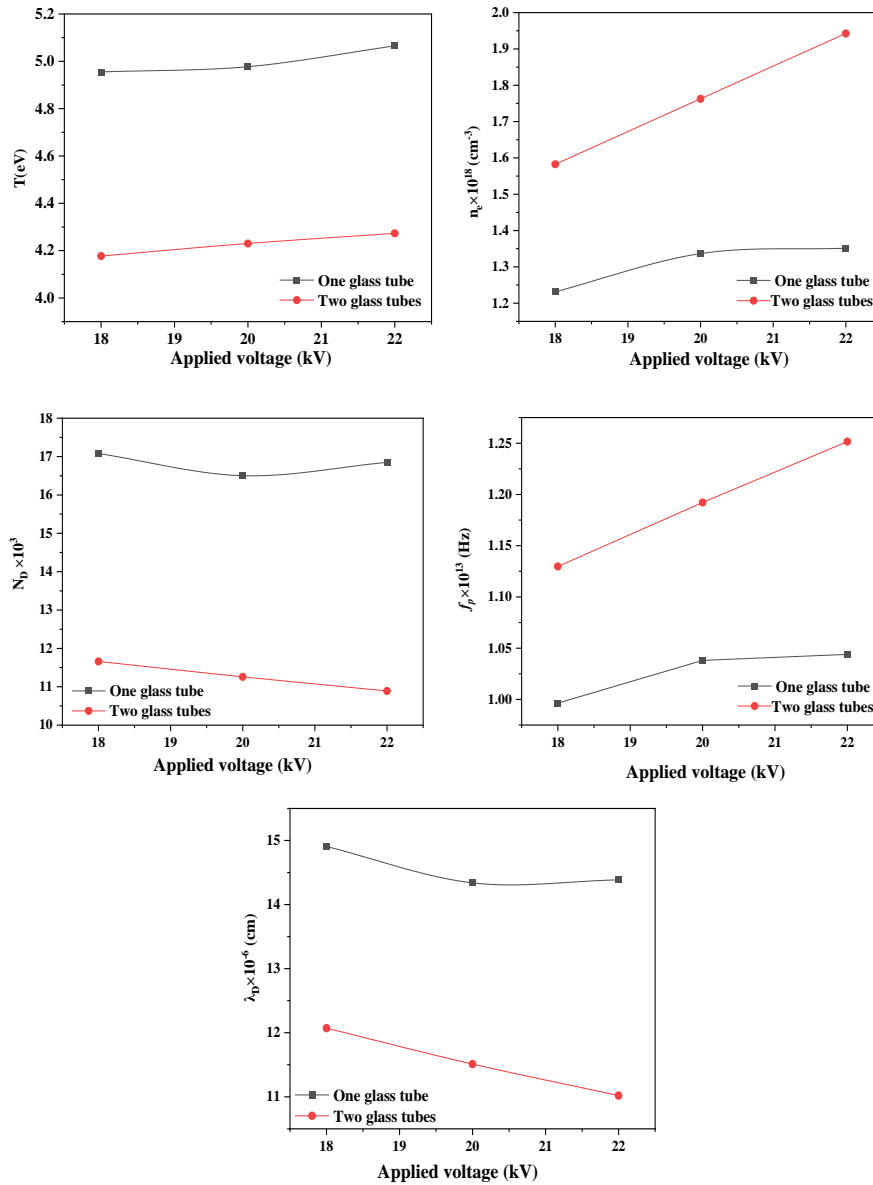


**Figure 10:** Effect of applied voltages on DBD plasma parameters both electrode designs.

Table 1 listed all the plasma parameters produced at different conditions of applied voltage and discharge gap distance for both designs.

**Table 1:** Plasma parameters at different voltages for one and two glass tube

Applied Voltage (kV)	ONE GLASS TUBE					TWO GLASS TUBES				
	$T_e$ (eV)	$n_e \times 10^{18}$ (cm <sup>-3</sup> )	$f_p \times 10^{13}$ (Hz)	$\lambda_D \times 10^{-5}$ (cm)	$N_D \times 10^3$	$T_e$ (eV)	$n_e \times 10^{18}$ (cm <sup>-3</sup> )	$f_p \times 10^{13}$ (Hz)	$\lambda_D \times 10^{-5}$ (cm)	$N_D \times 10^3$
18	4.955	1.23	0.996	1.490	17.07	4.177	1.582	1.129	1.207	11.65
20	4.977	1.78	1.038	1.433	16.50	4.23	1.762	1.192	1.151	11.25
22	5.065	1.85	1.043	1.438	16.84	4.273	1.942	1.251	1.101	10.88

## Conclusions

The specific design of the electrodes (one glass tube and two glass tubes) has a clear effect on the properties of the produced plasma; this effect appears as a change in the distribution and homogeneity of plasma intensity in the discharge gap between the discharge electrodes, as a result of formation an electric field with specific properties in this region based on electrodes configuration. Consequently, electron temperature plasma density and all plasma parameters will be sensitive to changes in electrode design.

## Acknowledgements

The authors are thankful for the support of Mustansiriyah University – Baghdad – Iraq ([www.uomustansiriyah.edu.iq](http://www.uomustansiriyah.edu.iq)).

## Reference

- [1] J. Julák, H. Soušková, V. Scholtz, E. Kvasničková, D. Savická, and V. Kříha, “Comparison of fungicidal properties of non-thermal plasma produced by corona discharge and dielectric barrier discharge,” *Folia Microbiol. (Praha)*, vol. 63, pp. 63–68, 2018.
- [2] K. D. Weltmann and T. Von Woedtke, “Plasma medicine—current state of research and medical application,” *Plasma Phys. Control. Fusion*, vol. 59, no. 1, p. 14031, 2016.
- [3] M. Hijosa-Valsero, R. Molina, and J. M. Bayona, “Assessment of a dielectric barrier discharge plasma reactor at atmospheric pressure for the removal of bisphenol A and tributyltin,” *Environ. Technol.*, vol. 35, no. 11, pp. 1418–1426, 2014.
- [4] Y. Hu, Y. Bai, H. Yu, C. Zhang, and J. Chen, “Degradation of selected organophosphate pesticides in wastewater by dielectric barrier discharge plasma,” *Bull. Environ. Contam. Toxicol.*, vol. 91, pp. 314–319, 2013.
- [5] H. Ghomi, S. Mohades, N. Navab Safa, and H. Dabiri, “Surface decontamination by dielectric barrier discharge plasma,” *J. Biomed. Phys. Eng.*, vol. 2, no. 2, 2012.
- [6] M. F. Figueroa-Pinochet *et al.*, “Dielectric Barrier Discharge for Solid Food Applications,” *Nutrients*, vol. 14, no. 21, p. 4653, 2022.
- [7] R. D’Agostino, P. Favia, C. Oehr, M. R. Wertheimer, and S. Kalveram, “Five years of excellence in plasma science,” *Plasma Processes and Polymers*, vol. 6, no. 1. Wiley Online Library, pp. 7–10, 2009.
- [8] Ahmed, R. Q. M. B. M., “Optical Diagnostics of Zn foil using Non thermal plasma jets (NTPJ) via high voltage”, *Mustansiriyah Journal of Pure and Applied Sciences*, vol.2, no.2, pp.112-125, (2024).
- [9] Y. Miao, A. Yokochi, G. Jovanovic, S. Zhang, and A. von Jouanne, “Application-oriented non-thermal plasma in chemical reaction engineering: A review,” *Green Energy Resour.*, vol. 1, no. 1, p. 100004, 2023.
- [10] J. Moszczyńska, K. Roszek, and M. Wiśniewski, “Non-thermal plasma application in medicine—

- Focus on reactive species involvement,” *Int. J. Mol. Sci.*, vol. 24, no. 16, p. 12667, 2023.
- [11] R. Barni, P. Alex, and C. Riccardi, “Pulsed Dielectric Barrier Discharges for Gas-Phase Composition Control: A Simulation Model,” *Plasma*, vol. 6, no. 4, pp. 735–752, 2023.
- [12] I. H. Hashim, A. K. L. Oudah, and B. J. Hussein, “Impact of Electrodes Material on the Properties of Atmospheric DBD Plasma,” *Iraqi J. Sci.*, pp. 4273–4280, 2023.
- [13] D. P. Subedi, “An investigation of the effect of electrode geometry and frequency of power supply in the homogeneity of dielectric barrier discharge in air,” *Kathmandu Univ. J. Sci. Eng. Technol.*, vol. 6, no. 1, pp. 96–101, 2010.
- [14] K. A. Aadim, S. N. Mazhir, N. K. Abdalameer, and A. H. Ali, “Influence of gas flow rate on plasma parameters produced by a plasma jet and its spectroscopic diagnosis using the OES technique,” in *IOP Conference Series: Materials Science and Engineering*, IOP Publishing, 2020, p. 12020.
- [15] N. Ohno, M. A. Razzak, H. Ukai, S. Takamura, and Y. Uesugi, “Validity of electron temperature measurement by using Boltzmann plot method in radio frequency inductive discharge in the atmospheric pressure range,” *Plasma fusion Res.*, vol. 1, p. 28, 2006.
- [16] R. N. Muhsin and K. A. Aadim, “Spectroscopic study performance of laser produced CdTe (x): S (plasma,” *Iraqi J. Phys.*, vol. 17, no. 42, pp. 96–102, 2019.
- [17] H. Q. Farag and S. J. Kadhem, “Study the Effect of Dielectric Barrier Discharge (DBD) Plasma on the Decomposition of Volatile Organic Compounds,” *Iraqi J. Phys.*, vol. 20, no. 4, pp. 45–53, 2022.
- [18] M. B. Kizling and S. G. Järås, “A review of the use of plasma techniques in catalyst preparation and catalytic reactions,” *Appl. Catal. A Gen.*, vol. 147, no. 1, pp. 1–21, 1996.
- [19] Y. Ralchenko, “NIST Atomic Spectra database (ver. 4.1. 0),” <http://physics.nist.gov/asd/>, 2011.
- [20] B. M. Goldberg, T. Hoder, and R. Brandenburg, “Electric field determination in transient plasmas: in situ & non-invasive methods,” *Plasma Sources Sci. Technol.*, vol. 31, no. 7, p. 73001, 2022.
- [21] N. Pourali, K. Lai, J. Gregory, Y. Gong, V. Hessel, and E. V. Rebrov, “Study of plasma parameters and gas heating in the voltage range of nondischarge to full-discharge in a methane-fed dielectric barrier discharge,” *Plasma Process. Polym.*, vol. 20, no. 1, p. 2200086, 2023.
- [22] R. Brandenburg, “Dielectric barrier discharges: progress on plasma sources and on the understanding of regimes and single filaments,” *Plasma Sources Sci. Technol.*, vol. 26, no. 5, p. 53001, 2017.